Proximal magnetometry of monolayers of single molecule magnets on gold using polarized muons

Z. Salman*
Clarendon Laboratory, Department of Physics, Oxford University, Parks Road, Oxford OX1 3PU, UK and Paul Scherrer Institute, Laboratory for Muon Spin Spectroscopy, CH-5232 Villigen PSI, Switzerland

S.J. Blundell
Clarendon Laboratory, Department of Physics, Oxford University, Parks Road, Oxford OX1 3PU, UK

S.R. Giblin
ISIS Facility, Rutherford Appleton Laboratory, Chilton, Oxfordshire, OX11 0QX, UK

M. Mannini
Dipartimento di Chimica, Università di Firenze & INSTM, via della Lastruccia 3, 50019 Sesto Fiorentino, Italy and ISTM-CNR, URT Firenze, 50019 Sesto Fiorentino, Italy.

L. Margheriti and R. Sessoli
Dipartimento di Chimica, Università di Firenze & INSTM, via della Lastruccia 3, 50019 Sesto Fiorentino, Italy

E. Morenzoni, T. Prokscha, and A. Suter
Paul Scherrer Institute, Laboratory for Muon Spin Spectroscopy, CH-5232 Villigen PSI, Switzerland

A. Cornia
Department of Chemistry & INSTM Research Unit, Università degli Studi di Modena e Reggio Emilia, Via G. Campi 183, 41100 Modena, Italy

The magnetic properties of a monolayer of Fe_4 single molecule magnets grafted onto a Au (111) thin film have been investigated using low energy muon spin rotation. The properties of the monolayer are compared to bulk Fe_4. We find that the magnetic properties in the monolayer are consistent with those measured in the bulk, strongly indicating that the single molecule magnet nature of Fe_4 is preserved in a monolayer. However, differences in the temperature dependencies point to a small difference in their energy scale. We attribute this to a $\sim 60\%$ increase in the intramolecular magnetic interactions in the monolayer.

A promising strategy to encode information in molecular units is provided by single molecule magnets (SMMs) [1], chemically identical nanoscale clusters of exchange-coupled transition metal or rare earth ions and associated ligands. SMMs have been used to study quantum tunneling of magnetization and topological quantum phase interference [2] and may find applications in quantum information processing [3, 4, 5]. The assembly of these systems on surfaces is currently investigated [6, 7, 8, 9, 10, 11, 12, 13] as this represents a necessary prerequisite for magnetic memory applications. Recently, synchrotron-based techniques have been used to confirm that Fe_4 SMMs remain intact when grafted on a gold surface preserving their unique magnetic properties [8]. However, the effect of the surface on an SMM is still not well understood. This is due to the small quantity of magnetic material contained in a (sub)monolayer which prevents the use of techniques such as SQUID magnetometry or conventional nuclear magnetic resonance (NMR). In this paper we overcome this obstacle by using a novel proximal magnetometry technique utilizing muons as an implanted local probe to investigate magnetic properties of a monolayer of Fe_4 molecules when they are grafted on a Au (111) substrate. We anticipate that this method will provide a powerful tool with a high sensitivity over a wide range of time scales and energies, thus improving our understanding of the influence of the surface on a grafted SMM.

To date, Fe_4 (Fig. 1) is the only SMM complex that has been clearly shown to maintain its SMM behaviour when grafted on a surface[8]. In the bulk it has a $S = 5$ ground state and a reversal anisotropy barrier up to 17 K[14]. In this work the properties of the monolayer measured using low energy muon spin rotation (LE-μSR) method (see below) are compared to conventional muon spin rotation (μSR) measurements in bulk Fe_4 powder samples. In both monolayer and bulk, the strength and distribution of the magnetic dipolar fields from the Fe_4 moments determine the muon spin precession and relaxation. Inter-

*Electronic address: zaher.salman1@psi.ch

estingly, the qualitative temperature dependence of the relaxation in both monolayer and bulk are similar, however, the temperature scales differ. These results are in agreement with previous X-ray absorption measurements (XAS) [8], namely they show that the general SMM nature of Fe_4 is preserved in the monolayer, in contrast with what is observed for the archetypal SMM Mn_{12} [15, 16]. Nevertheless, we detect modifications of the microscopic properties of SMMs compared to bulk that we attribute to an enhancement of the exchange interaction in the tetranuclear cluster. LE-μSR is thus confirmed as an exceptionally powerful tool for the investigation of magnetic nanostructures, providing a complementary view of their magnetic properties.

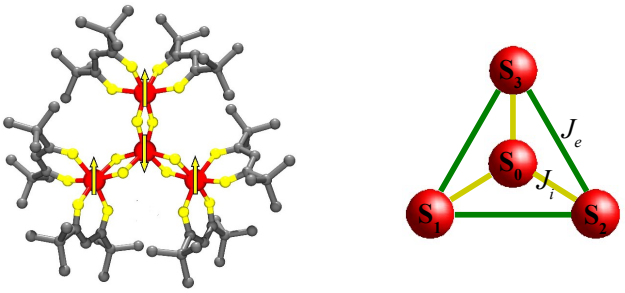

FIG. 1: (color online) A schematic view of the magnetic core of the Fe_4 single molecule magnet. The red balls denote Fe^{3+} ions while oxygen atoms are shown in yellow and carbon atoms in gray. On the right panel we show the labeling scheme of exchange interactions.

The LE-μSR experiments[17, 18] were performed on the low energy muons beamline at PSI in Switzerland. In these experiments 100% polarized positive muons are implanted in the sample. The studied samples were mounted in an ultra high vacuum (UHV) environment on a cold finger cryostat. The experiments described here were performed in the transverse field (TF) configuration, where the muon polarization is transverse to the direction of the beam and the applied magnetic field. Each implanted muon decays (lifetime $\tau = 2.2$ μs) emitting a positron preferentially in the direction of its polarization at the time of decay. Using appropriately positioned detectors, one measures the asymmetry of the muon beta decay along a certain direction as a function of time $A(t)$, which is proportional to the time evolution of the muon spin polarization, $P(t)$, along that direction. $A(t)$ depends on the distribution of internal magnetic fields and their temporal fluctuations. In LE-μSR experiments, the muons implantation energy can be varied between $1 - 32$ keV, corresponding to an average implantation depth of $5 - 200$ nm, allowing depth resolved LE-μSR measurements.

LE-μSR measurements on two samples are reported here; sample **1** is a monolayer of a Fe_4 (hereafter referred to as Fe_4^{ML}) grafted on a 200 nm thick Au(111) film through sulfur-functionalization[14, 19]. Sample **2** is an identically prepared bare Au(111) film, used as a control sample in order to confirm that the effects measured in **1** are solely due to the grafted Fe_4^{ML}. The functionalized Fe_4 cluster $[Fe_4(L^A)_2(dpm)_6]$, where Hdpm=dipivaloylmethane, and H_3L^A=11-(acetylthio)-2,2-bis(hydroxymethyl)undecan-1-ol, synthesized according to Ref. [19] has been used to prepare a monolayer on gold by a wet chemistry approach. This is based on a three-step process as described in Ref. [8]; 1) Hydrogen flame annealing of a ~ 200 nm thick Au film (evaporated on mica) to obtain a flat Au(111) surface, 2) incubating the annealed Au film in a solution of $[Fe_4(L^A)_2(dpm)_6]$ in CH_2Cl_2 for 20 hours to insure full coverage of the Au surface, and 3) repeated washing with CH_2Cl_2 to remove the excess of physisorbed molecules and drying the sample in nitrogen flow.

The temperature and magnetic field dependence of the LE-μSR precession signals in both samples were measured by implanting the muons at different energies in the Au film, *below* the Fe_4^{ML} monolayer. The magnetic field was applied perpendicular to the Au surface. These results are compared here to the bulk μSR measurements performed on sample **3** [20]; a powder sample of an unfunctionalized $[Fe_4(L^B)_2(dpm)_6]$ cluster, where H_3L^B is the commercially available tripodal ligand 1,1,1-tris(hydroxymethyl)ethane, prepared according to Ref. [21] (hereafter referred to as Fe_4^B). In the bulk, both functionalized and unfunctionalized Fe_4 clusters have very similar spin Hamiltonian parameters, in particular the nearest-neighbor exchange interaction between Fe spins are $J_i = 22.2 - 22.9$ K (depending on the crystal phase) [14, 19] and 23.8 K [21] for the functionalized and unfunctionalized clusters, respectively.

Typical LE-μSR precession signals recorded at $T = 6$ K and two different implantation energies (E) are shown in Fig. 2. The corresponding muon stopping profiles at 1.5 and 22.5 keV implantation energies are shown in Fig. 2(a). The muon polarization follows a precessing damping signal

$$P(t) = P_0 \cos(\omega t) e^{-\lambda t}, \quad (1)$$

where P_0 is the initial polarization, ω is the precession frequency and λ is the damping/relaxation rate of the oscillations. In these measurements, the precession frequency is $\omega = \gamma B$, where $\gamma = 135.5$ MHz/T is the muon gyromagnetic ratio and B is the average local magnetic field experienced by the muons. The relaxation rate λ gives a measure of the width of the distribution of local magnetic fields, thus a wider field distribution results in a larger λ. Note that this parameter is primarily a measure of the local static magnetic fields, but may also include small contributions from dynamic magnetic fields as well. In general, muons are sensitive to magnetic field fluctuations in the range $10^{-11} - 10^{-4}$ s. Faster fluctuations are averaged out while slower fluctuations are static over the lifetime of the muon (2.2 μs).

The average local field measured at all temperatures and implantation energies (in both samples **1** and **2**) was equal to the applied field, B_0. However, the distribution

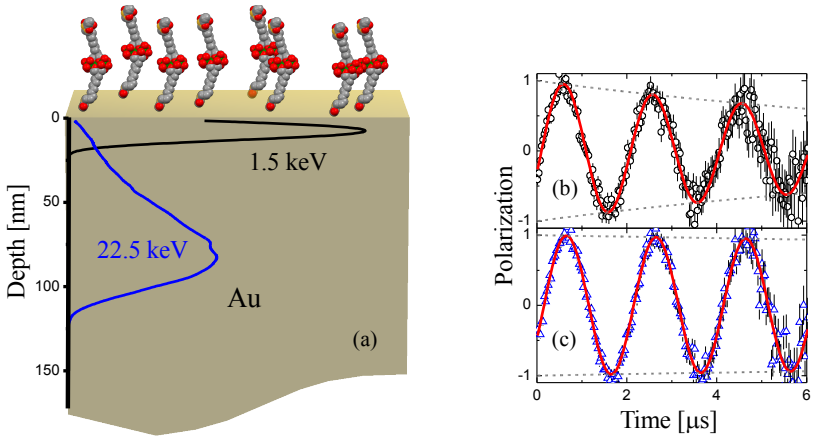

FIG. 2: (color online) (a) A schematic view of sample **1** where the Fe_4^{ML} molecules are grafted on the Au film. The stopping profiles of muons in Au at $E = 1.5$ and 22.5 keV are also shown. Typical muon spin precession spectra in the rotating reference frame measured in sample **1** at $T = 6$ K, $B_0 = 110$ mT and implantation energy (b) 1.5 keV and (c) 22.5 keV. The solid lines are fits to a damping precession signal and the dashed lines represent the damping amplitude.

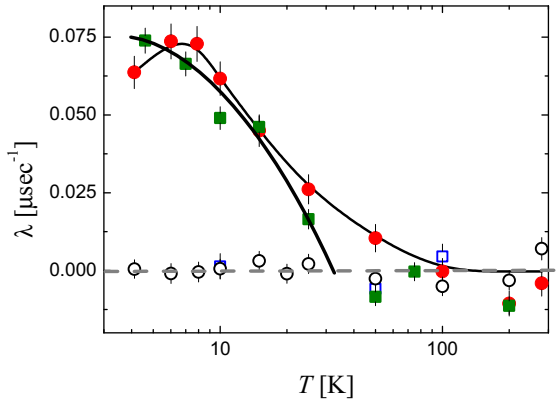

FIG. 3: (color online) The relative relaxation rate measured in sample **1** (full symbols) and **2** (open symbols). The squares and circles indicate measurements in $B_0 = 8.3$ mT and 110 mT, respectively. The lines are a guide to the eye.

of fields measured by λ exhibits a strong T and E dependence only in sample **1** but not in **2**. For example, in Fig. 2(b) we plot $P(t)$ at $E = 1.5$ keV, where most of the muons stop within $10 - 20$ nm of the Au surface, and the dipolar fields from the Fe_4^{ML} moments are large [15]. In contrast, in Fig. 2(c) we plot $P(t)$ at $E = 22.5$ keV where the average muon implantation depth is ~ 100 nm, and the dipolar fields at this depth are negligible. Therefore, the measured λ at 1.5 keV is larger than that at 22.5 keV. Note that the dipolar fields sensed by the implanted muons are proportional to the average size of the Fe_4^{ML} magnetic moment, which is determined by the population of the different spin states of Fe_4^{ML}[14, 19].

The strong temperature dependence of λ measured at low energy is shown in Fig. 3. Here we plot λ in sample **1** relative to **2**; i.e. zero relaxation is taken as the average relaxation measured in the reference sample (since there is no temperature and field dependence). Note that the precession signals measured in sample **2** are identical to those measured at high energy in sample **1** and do not depend on T or E.

At high temperatures ($T \gg J_i$) and $E = 1.5$ keV the relaxation rate is temperature independent and small (similar to sample **2**). This is due to fast thermal fluctuations of the individual Fe magnetic moments, which average out the dipolar magnetic field experienced by muons and therefore produces a narrower field distribution (smaller λ). Below $\sim 40 - 50$ K the relaxation rate increases rapidly with decreasing temperature, indicating a slowing down of the fluctuations of the Fe moments and an increase in the magnetic correlations within each molecule. Therefore, the average magnetic moment per molecule and hence the dipolar fields on the muons increase. At $B_0 = 110$ mT the relaxation rate peaks at ~ 6 K and then decreases upon further cooling, in contrast to the monotonic increase at $B_0 = 8.3$ mT. The difference between the temperature dependencies at different fields is due to the strong field dependence of the Fe_4 spin energy levels and its magnetic moment [14].

Similar bulk μSR measurements were done on a powder Fe_4^B sample, in the same temperature range and applied field transverse to the muon spin direction. In these measurements, we detect two precession signals due to two inequivalent muon sites. The temperature dependence of the precession parameters are qualitatively similar for both sites, and therefore we compare the measurements in the monolayer to the precession signal of the majority of the muons in bulk. The relaxation rates measured at $B_0 = 8.3$ and 110 mT are shown in Fig. 4(a) and (b), respectively, along with the corresponding data in Fe_4^{ML} . As in the case of the LE-μSR measurements, these relaxation rates are due to the distribution of dipolar fields in bulk at the respective applied fields. Therefore, the underlying mechanism of spin relaxation in both cases is identical.

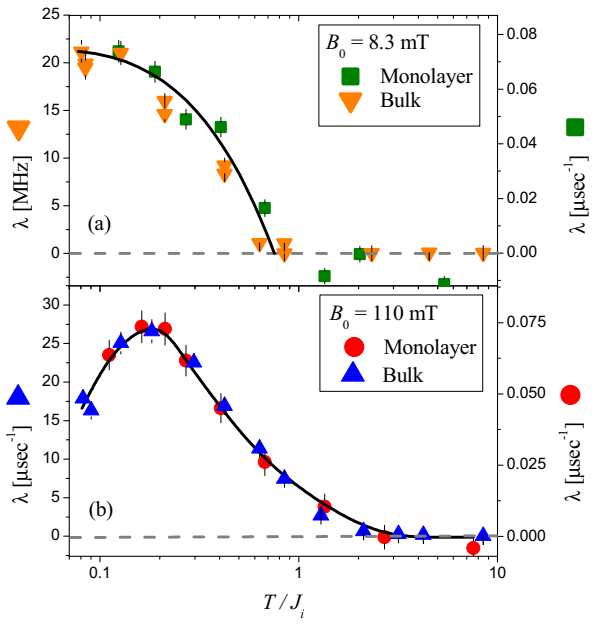

FIG. 4: (color online) The relaxation rate as a function of the normalized temperature measured in bulk Fe_4 compared to monolayer at fields (a) 8.3 and (b) 110 mT. The lines are a guide to the eye.

The observed temperature dependence of the relaxation rates is typical of molecular nanomagnets and reflects the building up of exchange correlations among the spins of the molecule, widely investigated using NMR and μSR [22, 23, 24]. As expected, the temperature dependencies measured in the monolayer have striking qualitative resemblance to those measured in bulk. However, the ratio of the relaxations in Fe_4^B:Fe_4^{ML} is $\sim$ 300 : 1 indicating that the muons in the monolayer are on average $\sim$ 7 times further from the Fe_4 moments compared to bulk, and therefore experience much smaller dipolar fields. Interestingly, the temperature dependence in the monolayer seems to be shifted to higher temperatures compared to bulk. This shift is almost logarithmic in temperature, indicating that it occurs due to a temperature independent increase in the energy scales of Fe_4^{ML} compared to Fe_4^B.

Given the sensitivity of muons to the energy spectrum arising from exchange interactions in magnetic molecules [22, 23, 24] we attempt to rationalize the observed shift by using the following spin Hamiltonian for Fe_4 [19]

$$\mathcal{H}_0 = J_i \mathbf{S}_0 \cdot \sum_{k=1}^{3} \mathbf{S}_k + J_e \left[\mathbf{S}_1 \cdot \mathbf{S}_2 + \mathbf{S}_2 \cdot \mathbf{S}_3 + \mathbf{S}_3 \cdot \mathbf{S}_1 \right], \quad (2)$$

where J_i is the super-exchange coupling between the central ($\mathbf{S}_0$) and the three peripheral ($\mathbf{S}_k$) Fe ions, and J_e is the next nearest neighbour interaction (Fig. 1). Since $J_i \gg J_e$ the landscape of total spin levels is determined mainly by J_i. In a simplified picture we interpret the temperature dependence of λ as follows. For $T \gg J_i$ the individual Fe magnetic moments are thermally fluctuating. These fluctuations slow down as T approaches J_i, and continue to do so at lower temperatures as correlations between the individual Fe moments within each molecule are formed. This is also accompanied by an increase in the average magnetic moment of the molecule. The increase observed in the relaxation rate is associated with the increase in dipolar fields due to the larger moments as well as the slowing down of the fluctuations [23, 24, 25]. Since J_i provides the basic energy scale in this system (at high temperatures), it is intuitive to plot the relaxation rate as a function of the normalized temperature, T/J_i (Fig. 4). For the Fe_4 clusters used here J_i^B evaluated from magnetic measurements is found to be 23 (1) K [14, 19, 21], and therefore the temperature dependence of the relaxation rate in Fe_4^B shows a dramatic increase below $T/J_i^B \sim 1$. In contrast, the value of the coupling J_i^{ML} in Fe_4^{ML} is unknown. However, in order to obtain a similar behaviour to that seen in bulk, one has to plot the relaxation rate in the monolayer against a normalized temperature T/J_i^{ML}, where $J_i^{ML} = 37(1)$ K. This clearly produces an excellent agreement between the relaxation rates measured in bulk and monolayer for all temperatures and magnetic fields, suggesting that the main difference between Fe_4 in bulk and monolayer can be accounted for by a $\sim$ 60% increase in J_i of Fe_4^{ML} over Fe_4^B. Enhancement in the Fe-Fe J coupling as a function of the Fe-O-Fe angle has been observed in iron dimers [26], and predicted using first principle density functional theory calculations [27]. We should also take into account that thermal fluctuations of the spins are governed by the spin-phonon coupling and sound velocity [28]. These are also expected to be dramatically altered by the different environment of the monolayer, and could result in the apparent change in energy scale. However, it is less likely that this effect plays a dominant role since it would not explain the observed scaling between monolayer and bulk.

In conclusion, our results have demonstrated that the general SMM nature of Fe_4 is preserved in the monolayer, in contrast to the case of Mn_{12}[15, 16]. The observation of a different temperature scale of the magnetic properties of the monolayer suggests an enhancement of the intramolecular interactions between the individual Fe ions within the Fe_4 core. This implies a non negligible role played by the surface, which, once understood, could be exploited to tune the magnetic properties of nanostructured SMMs. By using polarized muons as proximal magnetometers, we have developed a very powerful technique able to characterize the magnetic properties of exceedingly small amounts of magnetic molecules, over a wide range of time scales and energies. This capability opens the possibility to investigate the details of the effects of surfaces on the magnetic properties of molecular nanostructures, which is not possible using other conventional techniques.

This work was performed at the Swiss Muon Source SμS, Paul Scherrer Institute, Villigen, Switzerland. We

would like to thank Hans-Peter Weber for technical assistance and Giovanni Aloisi for the help in the preparation of gold substrates. The financial support of the EU through the NoE MAGMANet , and through NANOsci-ERA and MOLSPINQUIP projects is gratefully acknowledged.

[1] D. Gatteschi, R. Sessoli, *Angew. Chem. Int. Ed.* **42**, 268 (2003).
[2] W. Wernsdorfer, R. Sessoli, *Science* **284**, 133 (1999).
[3] J. Tejada, E. M. Chudnovsky, E. del Barco, J. M. Hernandez, T. P. Spiller, *Nanotechnology* **12**, 181 (2001).
[4] A. Ardavan, *et al.*, *Phys. Rev. Lett.* **98**, 057201 (2007).
[5] M. N. Leuenberger, D. Loss, *Nature* **410**, 789 (2001).
[6] A. Cornia, *et al.*, *Angew. Chem. Int. Ed.* **42**, 1645 (2003).
[7] G. G. Condorelli, *et al.*, *Angew. Chem. Int. Ed.* **43**, 4081 (2004).
[8] M. Mannini, *et al.*, *Nat Mater* **8**, 194 (2009).
[9] A. Naitabdi, J.-P. Bucher, P. Gerbier, P. Rabu, M. Drillon, *Adv. Mater.* **17**, 1612 (2005).
[10] J. Gomez-Segura, *et al.*, *Chem. Comm.* pp. 2866–2868 (2006).
[11] E. Coronado, *et al.*, *Inorg. Chem.* **44**, 7693 (2005).
[12] M. Burgert, *et al.*, *J. Am. Chem. Soc.* **129**, 14362 (2007).
[13] B. Fleury, *et al.*, *Chem. Commun.* p. 2020 (2005).
[14] L. Gregoli, *et al.*, *Chemistry - A European Journal* **15**, 6456 (2009).
[15] Z. Salman, *et al.*, *Nano Lett.* **7**, 1551 (2007).
[16] M. Mannini, *et al.*, *Chem. Eur. J.* **14**, 7530 (2008).
[17] E. Morenzoni, *et al.*, *Phys. Rev. Lett.* **72**, 2793 (1994).
[18] T. Prokscha, *et al.*, *Nucl. Instr. and Meth. A* **595**, 317 (2008).
[19] A. L. Barra, *et al.*, *European J. Inorg. Chem.* **26**, 4145 (2007).
[20] Z. Salman, *et al.*. The full characterization of sample **3** is out of the scope of this article and will be published elsewhere.
[21] A. Cornia, *et al.*, *Angew. Chem. Int. Ed.* **43**, 1136 (2004).
[22] F. Borsa, *NMR-MRI, μSR and Mossbauer spectroscopies in molecular magnets*, P. Carretta, A. Lascialfari, eds. (Spinger-Verlag, 2007).
[23] Z. Salman, *et al.*, *Phys. Rev. B* **65**, 132403 (2002).
[24] Z. Salman, *et al.*, *Phys. Rev. B* **77**, 214415 (2008).
[25] A. Lascialfari, Z. H. Jang, F. Borsa, P. Carretta, D. Gatteschi, *Phys. Rev. Lett.* **81**, 3773 (1998).
[26] F. L. Gall, *et al.*, *Inorg. Chim. Acta* **262**, 123 (1997).
[27] S. Stolbov, R. A. Klemm, T. S. Rahman, cond-mat/0501178.
[28] D. Gatteschi, R. Sessoli, J. Villain, *Molecular Nanomagnets* (Oxford University Press, 2006).